

Nonlocal Excitations and 1/8 Singularity in Cuprates

Yoshiro Kakehashi,* M. Atiqur R. Patoary, and Sumal Chandra

Department of Physics, University of the Ryukyus, Nishihara, Okinawa 903-0213, Japan

(To be published in the Journal of the Korean Physical Society)

Momentum-dependent excitation spectra of the two-dimensional Hubbard model on the square lattice have been investigated at zero temperature on the basis of the full self-consistent projection operator method in order to clarify nonlocal effects of electron correlations on the spectra. It is found that intersite antiferromagnetic correlations cause shadow bands and enhance the Mott-Hubbard splittings near the half-filling. Furthermore nonlocal excitations are shown to move the critical doping concentration δ_h^* , at which the singular quasiparticle peak is located just on the Fermi level, from $\delta_h^* = 0.153$ (the single-site value) to $\delta_h^* = 0.123$. The latter suggests the occurrence of an instability such as the stripe at $\delta_h^* = 1/8$.

PACS numbers: 71.10.-w, 71.18.+y, 74.72.-h

Keywords: single-particle excitations, momentum-dependent excitations, antiferromagnetic correlations, nonlocal excitations, Hubbard model, Mott-Hubbard bands, Fermi surface, cuprates, stripe instability

I. INTRODUCTION

Low energy excitations and associated unusual behaviors of electrons in two-dimensional copper-oxide superconductors have been a question under debates in the past quarter century. Although theoretical studies based on the quantum Monte-Carlo (QMC) [1], the exact diagonalization [2], and the other methods such as the dynamical cluster approximation (DCA) [3, 4] have clarified many aspects of the cuprate superconductors, the problems on the low energy excitations such as the non Fermi liquid behavior and the pseudogap state remain unresolved theoretically because of the limited range of the inter-site correlations and the limitation of the momentum and energy resolutions in the numerical calculations.

In order to describe long-range intersite correlations with high resolution in energy and momentum space, we have recently proposed a full self-consistent projection operator method (FSCPM) for single-particle excitations [5]. The theory is based on the projection operator technique for the retarded Green function, and makes use of an off-diagonal effective medium to describe the nonlocal correlations efficiently. The off-diagonal matrix elements of the effective medium are determined to be consistent with those of the self-energy of the Green function. We demonstrated on the basis of the half-filled Hubbard model on the simple cubic lattice that the long-range antiferromagnetic correlations cause shadow bands in the low-energy region and sub-peaks of the Mott-Hubbard bands in the strong interaction regime.

In this proceedings, we apply the theory to the two-dimensional Hubbard model which is the simplest model of the cuprates, and investigate nonlocal effects on the momentum-dependent single-particle excitation spectra at zero temperature. We will demonstrate that the

FSCPM describes well low-energy excitations of the doped two-dimensional Hubbard model with high resolutions and that the nonlocal correlations can cause the shadow bands as well as the shift of the Mott-Hubbard band splitting in the strong correlation regime. In particular, we suggest that a Fermi surface instability should take place at the doping concentration $\delta_h^* = 0.123$. This might correspond to the 1/8 instability of cuprates.

In the following section, we briefly review the FSCPM theory of single-particle excitations. In the theory we start from the Laplace transform of the retarded Green function. Introducing an off-diagonal effective medium, we expand the memory function with use of the incremental cluster expansion [6]. A remarkable point is that the off-diagonal effective medium is self-consistently taken into account up to the infinity so that high resolution is achieved in both energy and momentum. In Sec. III, we present numerical results of momentum dependent excitation spectra of the doped Hubbard model. In the last section we summarize a conclusion of the present work.

II. SELF-CONSISTENT PROJECTION OPERATOR APPROACH

We consider the retarded Green function, and adopt the Hubbard Hamiltonian H with nearest-neighbor transfer integral t and intra-atomic Coulomb interaction U . In the projection operator method [7], the retarded Green function $G_{ij\sigma}(z)$ is expressed with use of the Laplace transformation as follows.

$$G_{ij\sigma}(z) = \left(a_{i\sigma}^\dagger \left| \frac{1}{z-L} a_{j\sigma}^\dagger \right. \right). \quad (1)$$

Here the inner product between two operators A and B is defined by $(A|B) = \langle [A^+, B]_+ \rangle$, $\langle \cdot \rangle$ ($[\cdot, \cdot]_+$) being the thermal average (the anti-commutator). $a_{i\sigma}^\dagger$ ($a_{i\sigma}$) is the creation (annihilation) operator for an electron with spin σ on site i . Furthermore z denotes the complex

*Electronic address: yok@sci.u-ryukyu.ac.jp

energy variable $z = \omega + i\delta$ with δ being an infinitesimal positive number, and L is a Liouville operator defined by $LA = [H, A]_-$ for an operator A . Here $[,]_-$ is the commutator.

The Green function is expressed as follows according to the Dyson equation.

$$G_{ij\sigma}(z) = [(z - \mathbf{H}_0 - \mathbf{\Lambda}(z))^{-1}]_{ij\sigma}. \quad (2)$$

Here $(\mathbf{H}_0)_{ij\sigma}$ is the Hartree-Fock Hamiltonian matrix and $(\mathbf{\Lambda}(z))_{ij\sigma} = \Lambda_{ij\sigma}(z) = U^2 \bar{G}_{ij\sigma}(z)$ is the self-energy matrix. Reduced memory function $\bar{G}_{ij\sigma}(z)$ is given by

$$\bar{G}_{ij\sigma}(z) = \left(A_{i\sigma}^\dagger \left| \frac{1}{z - \bar{L}} A_{j\sigma}^\dagger \right. \right). \quad (3)$$

The operator $A_{i\sigma}^\dagger$ is defined by $A_{i\sigma}^\dagger = a_{i\sigma}^\dagger \delta n_{i-\sigma}$ with $\delta n_{i-\sigma} = n_{i-\sigma} - \langle n_{i-\sigma} \rangle$, and $\langle n_{i\sigma} \rangle$ is the average electron number on site i for spin σ . \bar{L} is a Liouville operator acting on the space orthogonal to the space $\{|a_{i\sigma}^\dagger\rangle\}$; $\bar{L} = QLQ$, $Q = 1 - P$, and $P = \sum_{i\sigma} |a_{i\sigma}^\dagger\rangle \langle a_{i\sigma}^\dagger|$.

In the FSCPM theory, we introduce an energy-dependent Liouville operator $\tilde{L}(z)$ for an effective Hamiltonian with an off-diagonal medium $\tilde{\Sigma}_{ij\sigma}(z)$; $\tilde{H}_0(z) = H_0 + \sum_{ij\sigma} \tilde{\Sigma}_{ij\sigma}(z) a_{i\sigma}^\dagger a_{j\sigma}$. Here H_0 is the Hartree-Fock Hamiltonian. The Green function $F_{ij\sigma}(z)$ for the Liouvillean $\tilde{L}(z)$ is expressed as

$$F_{ij\sigma}(z) = [(z - \mathbf{H}_0 - \tilde{\Sigma}(z))^{-1}]_{ij\sigma}, \quad (4)$$

where $(\tilde{\Sigma}(z))_{ij\sigma} = \tilde{\Sigma}_{ij\sigma}(z)$. It should be noted that the Green function $F_{ij\sigma}(z)$ becomes identical with $G_{ij\sigma}(z)$ when

$$\tilde{\Sigma}_{ij\sigma}(z) = \Lambda_{ij\sigma}(z). \quad (5)$$

In order to obtain an explicit expression of the self-energy $\Lambda_{ij\sigma}(z)$, we separate the Liouvillean L into $\tilde{L}(z)$ and the remaining interaction part $L_1(z)$, *i.e.*, $L = \tilde{L}(z) + L_1(z)$, and expand the memory function (3) with respect to the interaction by using the incremental method [6]. In the present calculations, we take into account the intersite correlations within the pair-site approximation;

$$\bar{G}_{ii\sigma}(z) = \bar{G}_{ii\sigma}^{(i)}(z) + \sum_{l \neq i} \Delta \bar{G}_{ii\sigma}^{(il)}(z), \quad (6)$$

$$\bar{G}_{ij\sigma}(z) = \bar{G}_{ij\sigma}^{(ij)}(z). \quad (7)$$

Here $\Delta \bar{G}_{ii\sigma}^{(il)}(z) = \bar{G}_{ii\sigma}^{(il)}(z) - \bar{G}_{ii\sigma}^{(i)}(z)$. These terms are calculated from cluster memory functions defined by $\bar{G}_{ij\sigma}^{(c)}(z) = (A_{i\sigma}^\dagger | (z - \bar{L}^{(c)}(z))^{-1} A_{j\sigma}^\dagger)$ ($c = i, ij$). $\bar{L}^{(c)}(z) = QL^{(c)}(z)Q$ and $L^{(c)}(z)$ is the Liouvillean for a cluster c embedded in the off-diagonal medium $\{\tilde{\Sigma}_{lm\sigma}(z)\}$.

In the calculation of the cluster memory functions mentioned above, we applied the form obtained by the renormalized perturbation theory [8].

$$\bar{G}_{ij\sigma}^{(c)}(z) = \left[\bar{G}_0^{(c)}(z) \cdot (1 - \bar{L}_I^{(c)} \cdot \bar{G}_0^{(c)}(z))^{-1} \right]_{ij\sigma}. \quad (8)$$

Here $(\bar{L}_I^{(c)})_{i\sigma j\sigma'} = U(1 - 2\langle n_{i-\sigma} \rangle) / \chi_{i\sigma}$, and $\chi_{i\sigma} = \langle n_{i-\sigma} \rangle (1 - \langle n_{i-\sigma} \rangle)$. In the simplest approximation [8], $(\bar{G}_0^{(c)})_{ij\sigma}(z)$ is given by

$$(\bar{G}_0^{(c)})_{ij\sigma}(z) = A_{ij\sigma} \int \frac{d\epsilon d\epsilon' d\epsilon'' \rho_{ij\sigma}^{(c)}(\epsilon) \rho_{ij-\sigma}^{(c)}(\epsilon') \rho_{ji-\sigma}^{(c)}(\epsilon'') \chi(\epsilon, \epsilon', \epsilon'')}{z - \epsilon - \epsilon' + \epsilon''}. \quad (9)$$

Here $A_{ij\sigma} = [\chi_{i\sigma} / \langle n_{i-\sigma} \rangle_c (1 - \langle n_{i-\sigma} \rangle_c)] \delta_{ij} + 1 - \delta_{ij}$, $\chi(\epsilon, \epsilon', \epsilon'') = (1 - f(\epsilon))(1 - f(\epsilon'))f(\epsilon'') + f(\epsilon)f(\epsilon')(1 - f(\epsilon''))$, $f(\epsilon)$ is the Fermi distribution function, $\langle n_{i\sigma} \rangle_c$ is the electron number for a cavity state defined by $\langle n_{i\sigma} \rangle_c = \int d\epsilon \rho_{ii\sigma}^{(c)}(\epsilon) f(\epsilon)$, and $\rho_{ij\sigma}^{(c)}(\epsilon) = -\pi^{-1} \text{Im}[(\mathbf{F}_c(z))^{-1} + \tilde{\Sigma}^{(c)}(z)]^{-1}]_{ij\sigma}$. The coherent cluster Green function $(\mathbf{F}_c(z))_{ij\sigma} = F_{ij\sigma}(z)$ is given by Eq. (4), and $(\tilde{\Sigma}^{(c)}(z))_{ij\sigma} = \tilde{\Sigma}_{ij\sigma}(z)$ for sites (i, j) belonging to the cluster c . Note that a ‘‘cluster’’ $c = (ij)$ does not mean that sites (i, j) are nearest neighbors. Instead they may be far apart.

Since we have truncated the higher-order terms in the expansions (6) and (7), the self-energy $\Lambda_{ij\sigma}(z) = U^2 \bar{G}_{ij\sigma}(z)$ depends on the medium $\tilde{\Sigma}_{ij\sigma}(z)$. We determine the medium self-consistently from condition (5). Note that the present theory reduces to the projection operator CPA in infinite dimensions [9], which is equivalent to the dynamical mean-field theory [10–12].

The momentum dependent excitation spectra are calculated from the Green function

$$G_{k\sigma}(z) = \frac{1}{z - \epsilon_{k\sigma} - \Lambda_{k\sigma}(z)}. \quad (10)$$

Here $\epsilon_{k\sigma}$ is the Hartree-Fock one-electron energy eigen value, and the momentum-dependent self-energy is calculated via Fourier transform of the off-diagonal self-energy as $\Lambda_{k\sigma}(z) = \sum_j \Lambda_{j0\sigma}(z) \exp(i\mathbf{k} \cdot \mathbf{R}_j)$. Note that the theory yields the spectra with high resolution in both energy and momentum because it is based on the retarded Green function and the off-diagonal effective medium is taken into account up to infinity in distance. In the DCA, the spectra with high resolution are not obtained at low temperatures because it relies on the numerical analytic continuation and a small size of cluster embedded in an effective medium.

III. NUMERICAL RESULTS

We have performed the self-consistent calculations of excitation spectra for the two-dimensional Hubbard model on the square lattice in the nonmagnetic state at zero temperature. In the calculations of the memory functions (9), we adopted the Laplace transform, and calculated off-diagonal self-energies up to the 50th nearest neighbors self-consistently.

Figure 1 shows calculated single-particle densities of states (DOS) for $U = 8$ in unit of $|t| = 1$ at half-filling. Note that the Mermin-Wagner theorem [13] tells

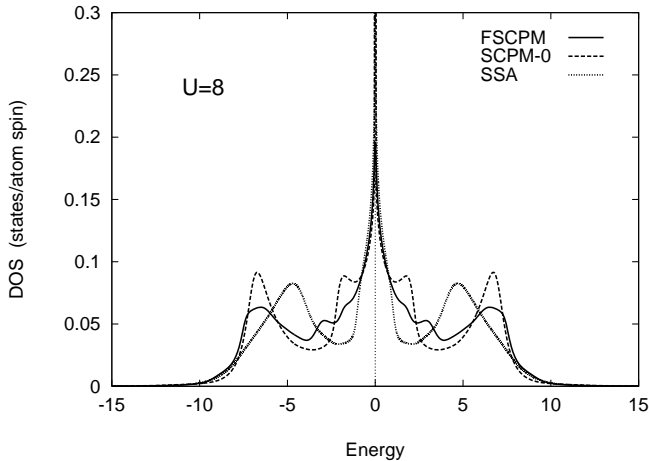


FIG. 1: The single-particle DOS at half-filling in the FSCPM (solid curve), the SCPM-0 (dashed curve), and the SSA (dotted curve).

us the antiferromagnetic state with the Néel temperature $T_N = 0$ K at half-filling, while we assumed here the nonmagnetic state. Thus the results presented here are not directly applicable at half-filling, but express the basic behavior of excitations in the vicinity of half-filling. The DOS is compared with those of the single-site approximation (SSA) and the diagonal self-consistent approximation (SCPM-0) in which the off-diagonal effective medium has been neglected, but the off-diagonal self-energies $\Lambda_{ij\sigma}(z)$ have been taken into account. The result indicates that the van Hove singularity remains near the Fermi level in the vicinity of half-filling. We find that nonlocal correlations increase the splitting between the upper and lower Hubbard bands as compared with the SSA. On the other hand, the peaks of the both Hubbard bands are suppressed as compared with those obtained by the SSA and the SCPM-0. The increment of the splitting is explained by strong antiferromagnetic correlations. In fact the latter cause the splitting $U + 2z_{NN}|J|$ instead of U in the strong correlation regime. Here z_{NN} is the number of the nearest neighbors, and J is the super-exchange interaction $J = -4|t|^2/U$. The formula yields the splitting 12, and explains the splitting in Fig. 1.

Nonlocal correlations also cause small peaks at energy $|\omega| \approx 3.0$. This is interpreted as shadow bands of type $\epsilon_{\pm}^{\text{SDW}}(k) = \pm\sqrt{\tilde{\epsilon}_k^2 + \Delta^2}$ due to long-range antiferromagnetic correlations. Here $\tilde{\epsilon}_k$ is a quasiparticle band, Δ is an exchange splitting.

When holes are doped, the spectral weight of the lower Hubbard band moves to the quasiparticle band as well as the upper Hubbard band. Furthermore the upper Hubbard band shifts to the higher energy region. Figure 2 shows an example of the momentum dependent excitation spectra in the optimum doped region. The excitations of the lower Hubbard band are damped, and those of the upper Hubbard band are enhanced. These re-

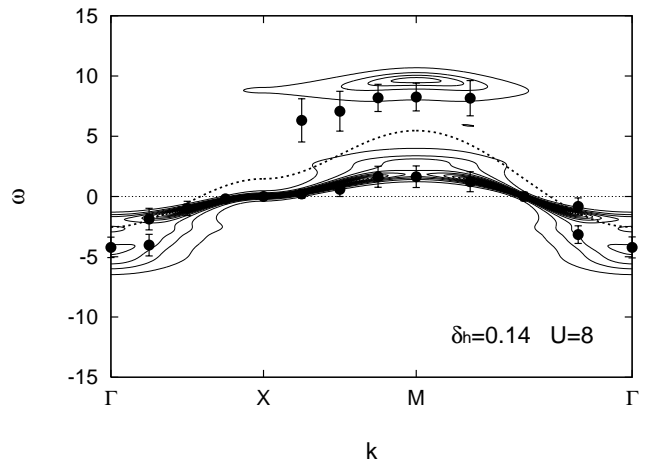


FIG. 2: Contour map of the momentum-dependent excitations along the high-symmetry lines at $\delta_h = 0.14$. Closed circles with error bars are the QMC results at $T = 0.33$. Dashed curve shows the Hartree-Fock quasiparticle dispersion.

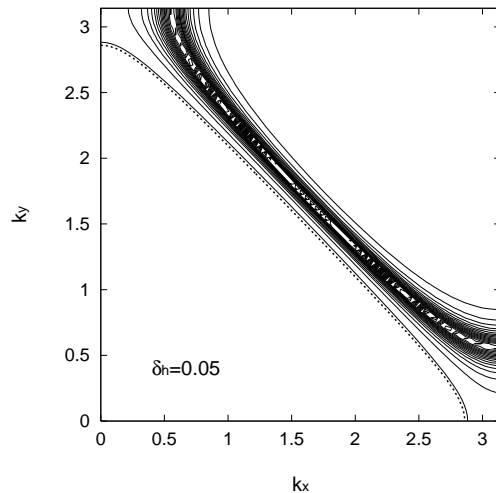


FIG. 3: Excitation spectrum at the Fermi energy for $\delta_h = 0.05$. The dotted curve shows the Fermi surface in the Hartree-Fock approximation.

sults of spectra are consistent with those of the QMC [1]. Especially, the quasiparticle band near the Fermi level shows a good agreement with that of the QMC.

Excitations at energy $\omega = 0$ determine the Fermi surface. We present in Figs. 3 and 4 the spectra at zero energy in the underdoped region ($\delta_h = 0.05$) as well as the overdoped region ($\delta_h = 0.20$). Due to a strong damping of the lower Hubbard band, a hole-like Fermi surface appears in the underdoped region, while in the overdoped region an electron-like Fermi surface appears. The results are in good agreement with those based on the QMC combined with the DCA [3].

Although the results of the FSCPM are consistent with those expected from the QMC+DCA at finite tem-

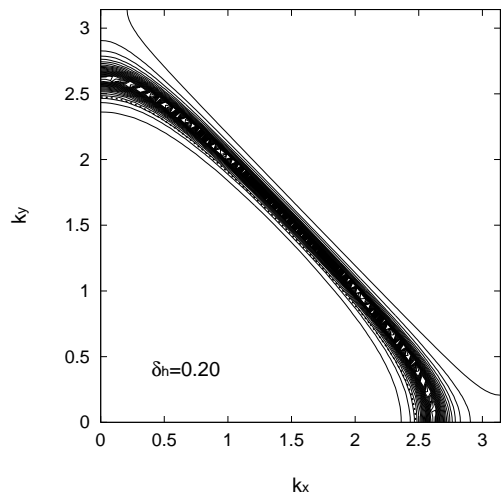


FIG. 4: Excitation spectrum at the Fermi energy for $\delta_h = 0.20$. The dotted curve shows the Fermi surface in the Hartree-Fock approximation.

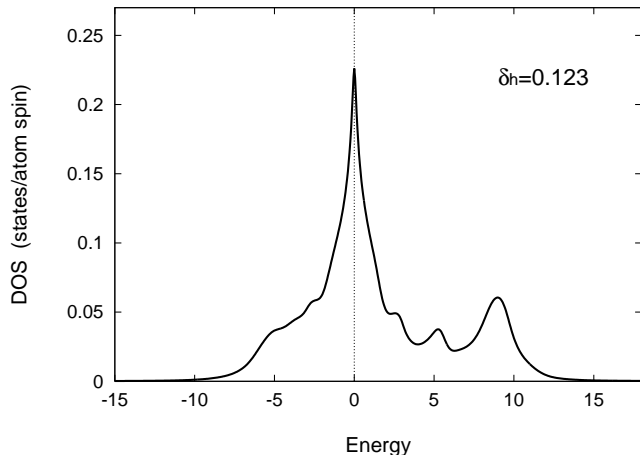


FIG. 5: The density of states at $\delta_h = 0.123$ where the quasiparticle peak is just on the Fermi level.

peratures, there are a few points showing the discrepancy. The marginal Fermi liquid behavior is one of them. The marginal Fermi liquid is characterized by the imaginary part of the self-energy being proportional to $\max(|\omega|, T)$ [14]. In the recent 4×4 QMC+DCA calculations [15], the marginal Fermi liquid behaviors are found at finite temperatures. The result for $U = 6$ suggests that the marginal Fermi liquid remains even at zero temperature at doping concentration $\delta_h^* = 0.15$, where the peak of the single-particle DOS is just on the Fermi level. This is rather close to the result of the SSA, $\delta_h^* = 0.153$ in our calculation (*i.e.*, the projection operator CPA).

We point out that the peak at δ_h^* is connected to that in Fig. 1 at zero doping. With the hole doping, the peak with van Hove singularity sinks first below the Fermi level

because of the transfer of the spectral weight from the lower Hubbard band to the upper Hubbard band. But, it gradually approach to the Fermi level with further doping, and the peak is again located on the Fermi level at δ_h^* .

In the present calculations of the FSCPM, the critical doping concentration at which the quasiparticle peak is located just on the Fermi level is $\delta_h^* = 0.123$ for $U = 8$ as shown in Fig. 5. Furthermore electrons are the Fermi liquid instead of the marginal Fermi liquid at δ_h^* because we find that the imaginary part of the momentum dependent self-energy in the quasiparticle energy region is proportional to ω^2 instead of $|\omega|$. It is remarkable that the critical concentration $\delta_h^* = 0.123$ is close to the 1/8 stripe instability found in the experiments [16, 17]. Though the present results indicate the Fermi liquid behavior, it is possible that the Fermi surface causes an instability at δ_h^* because of the peak just on the Fermi level, so that the normal state may change to the stripe phase at $\delta_h^* = 1/8$.

IV. CONCLUSION

We have investigated the nonlocal effects of electron correlations on the excitation spectra of the two-dimensional Hubbard model at zero temperature on the basis of the full self-consistent projection operator method (FSCPM). The FSCPM takes into account the long-range intersite correlations in a self-consistent way making use of the off-diagonal effective medium, and yields the spectra with high energy and momentum resolution. In the strong Coulomb interaction regime (*i.e.*, the case of $U = 8$), we found that the long-range intersite antiferromagnetic correlations create the shadow band excitations. The strong antiferromagnetic correlations also enhance the Mott-Hubbard splitting by about $2z_{NN}|J|$ where z_{NN} (J) is the number of the nearest neighbors (the super-exchange interactions energy). By comparing with the QMC and the QMC+DCA results, we verified that the FSCPM quantitatively describe the momentum dependent excitation spectra in the doped region. We also found that the nonlocal correlations shift the critical concentration δ_h^* at which the quasiparticle peak is located just on the Fermi level from $\delta_h^* = 0.153$ (the SSA) to $\delta_h^* = 0.123$, while the QMC+DCA at finite temperatures suggest $\delta_h^* = 0.15$ at zero temperature. Furthermore the electrons at $\delta_h^* = 0.123$ obtained by the FSCPM are the Fermi liquid, though the QMC+DCA suggested the marginal Fermi liquid even at zero temperature. It is plausible that the Fermi surface instability takes place because of the singular peak on the Fermi level. We speculate that such an anomaly corresponds to the 1/8 stripe instability and that it may cause the non Fermi liquid behaviors at finite temperatures as found in the QMC+DCA in the vicinity of δ_h^* . Details of the DOS and δ_h^* as a function of the Coulomb interaction U will be published elsewhere. Theoretical calculations for possible instabilities at δ_h^* are left for future investigations.

Acknowledgments

The authors would like to express their sincere thanks to Prof. Peter Fulde for valuable discussions. This work

is supported by a Grant-in-Aid for Scientific Research (22540395).

-
- [1] C. Gröber, R. Eder, and W. Hanke, Phys. Rev. B **62**, 4336 (2000).
 - [2] E. Dagotto, Rev. Mod. Phys. **66**, 763 (1994).
 - [3] Th. A. Maier, Th. Pruschke, and M. Jarrell, Phys. Rev. B **66**, 075102 (2002).
 - [4] T. Maier, M. Jarrell, T. Pruschke, and M.H. Hettler, Rev. Mod. Phys. **77**, 1027 (2005).
 - [5] Y. Kakehashi, T. Nakamura, and P. Fulde, J. Phys. Soc. Jpn. **78**, 124710 (2009).
 - [6] J. Gräfenstein, H. Stoll, and P. Fulde, Phys. Rev. B **55**, 13588 (1997).
 - [7] See for example, P. Fulde, *Electron Correlations in Molecules and Solids* (Springer, Berlin, 1995).
 - [8] Y. Kakehashi and P. Fulde, Phys. Rev. B **70**, 195102 (2004).
 - [9] Y. Kakehashi and P. Fulde, Phys. Rev. B **69**, 045101 (2004).
 - [10] S. Hirooka and M. Shimizu, J. Phys. Soc. Jpn. **43**, 70 (1977).
 - [11] A. Georges, G. Kotliar, W. Krauth, and M.J. Rosenberg, Rev. Mod. Phys. **68**, 13 (1996).
 - [12] Y. Kakehashi, Adv. Phys. **53**, 497 (2004).
 - [13] N.D. Mermin and H. Wagner, Phys. Rev. Lett **17**, 1133 (1966); D.K. Gohsh, Phys. Rev. Lett. **27**, 1584 (1971) [Errata; **28**, 3301 (1972)].
 - [14] C. M. Varma, P. B. Littlewood, S. Schmitt-Rink, E. Abrahams, and A. E. Ruckenstein, Phys. Rev. Lett. **63**, 1996 (1989); E. Abrahams and C. M. Varma, Phys. Rev. B **68**, 094502 (2003).
 - [15] N. S. Vidhyadhiraja, A. Macridin, C. Sen, M. Jarrell, and Michael Ma, Phys. Rev. Lett. **102**, 206407 (2009).
 - [16] A. R. Moodenbaugh, Y. Xu, M. Suenaga, T. J. Folkerts, R. N. Shelton, Phys. Rev. B **38**, 4596 (1988).
 - [17] T. Wu, H. Mayaffre, S. Krämer, M. Horvatić, C. Berthier, W. N. Hardy, R. Liang, D. A. Bonn, M. H. Julien, Nature **477**, 191 (2011).